**Biotransformation of hexachlorocyclohexanes contaminated biomass for**

**energetic utilization demonstrated in continuous anaerobic digestion system**

Shujuan Lian[a], Marcell Nikolausz*[b], Ivonne Nijenhuis[a], Ulisses Nunes da Rocha[b], Bin Liu[b],

Felipe Borim Corrêa[b], João Pedro Leonor Fernandes Saraiva[b] and Hans Hermann Richnow*[a]

[a] Department of Isotope Biogeochemistry, Helmholtz Centre for Environmental Research - UFZ,

Permoserstraße 15, 04318 Leipzig, Germany

(E-mail: shujuan.lian@ufz.de, ivonne.nijenhuis@ufz.de, hans.richnow@ufz.de)

[b] Department of Environmental Microbiology, Helmholtz Centre for Environmental Research -

UFZ, Permoserstraße 15, 04318 Leipzig, Germany

(E-mail: marcell.nikolausz@ufz.de, ulisses.rocha@ufz.de, bin.liu@ufz.de, felipe.correa@ufz.de,

joao.saraiva@ufz.de)

*Corresponding authors:

Hans Hermann Richnow, Tel.: +49 341 2351 212; E-mail: hans.richnow@ufz.de

Marcell Nikolausz, Tel.: +49 341 243 4566; E-mail: marcell.nikolausz@ufz.de

1

18 **Abstract**

19 Lindane, the γ-hexachlorocyclohexane (HCH) isomer, was among the most used pesticides

20 worldwide. Although it was banned in 2009, residues of Lindane and other HCH-isomers are still

21 found with high concentrations in contaminated fields. For clean-up, phytoremediation combined

22 with anaerobic digestion (AD) of contaminated biomass to produce biogas and fertilizer could be

23 a promising strategy and was tested in two 15 L laboratory-scale continuous-stirred-tank-

24 reactors. During operation over one year by adding HCH isomers (γ, α and β) consecutively, no

25 negative influence on conventional reactor parameters was observed. The γ- and α-HCH isomers

26 were transformed to chlorobenzene and benzene, and transformation became faster along with

27 time, while β-HCH was not removed. Genus *Methanosaeta* and order *Clostridiales*, showing

28 significant enhancement on abundance with HCH addition, may be used as bioindicators for

29 HCH dehalogenation in AD process. The potential for HCH degradation in AD system was

30 restricted to axial Cl atoms of HCH and it showed slight enantioselective preference towards

31 transformation of (+) α-HCH. Moreover, metabolite benzene was mineralized to $CO_2$ and

32 methane, deducing from tracer experiments with benzene-$^{13}C_6$. Overall, AD appears to be a

33 feasible option for treatment of γ and α-HCHs contaminated biomass.

34

35 **Key words:** Hexachlorocyclohexane; anaerobic digestion; stable isotope; reductive

36 dehalogenation; cleanup strategy

2

## 1. Introduction

Contamination by Persistent Organic Pollutants (POPs) prevents further utilization of arable lands for food and feed production. However, such lands may still be utilized for growth of energy crops with degradation properties such as wheat or other plants [1,2]. Potentially the contaminated biomass can be used as feedstock for anaerobic digestion (AD) to produce biogas as energy carrier and for use of the digestate as fertilizer. Thus, we propose a strategy combing phytoremediation with AD of hexachlorocyclohexane (HCH) contaminated biomass to produce biogas and still retain soil fertility, which might be a model for other halogenated POPs.

Huge amounts of Lindane, $\gamma$-HCH, have been used as pesticide worldwide until banned in the Stockholm convention 2009, due to the toxic and carcinogenic effects on human health and adverse environmental issues [3]. However HCHs are still found at high concentrations worldwide in areas of former pesticide production, since other HCH-isomers as by-products of Lindane production were dumped at production sites [4]. Plants and crops grown on contaminated land can accumulate HCH [5], which is a potential entry of HCH to food webs. Concentration between 1 and 10 $\mu$g g$^{-1}$ dry weight plant biomass has been found in the vicinity contaminated site [2] which is far above the acceptable levels and raises concerns when used as a food stock. However, contaminated biomass after phytoremediation [6,7] might be used for biogas production and opens an option for using polluted land [8]. Therefore, for clean-up, phytoremediation can be used in the contaminated field and the HCH-contaminated biomass can be used as substrate of AD for biogas production.

An understanding on the fate of HCHs in AD is required for the full-scale application. Anaerobic degradation processes metabolize pollutants through reductive pathways with mineralization or

3

59  reduction of highly electrophilic halo- and nitro-groups, to less toxic compounds by transferring

60  electrons to the contaminant [9–11]. Particularly reductive dehalogenation is favored under

61  anoxic conditions. Thus, HCH as persistent halogenated organic contaminants can be

62  transformed through reductive dehalogenation under anaerobic condition [12–16] and also in

63  biogas system as it was demonstrated in our recent study [8].

64  The transformation of HCHs during wastewater treatment in up-flow anaerobic sludge blanket

65  reactor (UASB) had been also reported [17,18]. However, the fate of HCH during continuous

66  large-scale AD with plant biomass feedstock and its effect on reactor performance during biogas

67  production was not yet investigated. According to our previous study with batch reactors [8],

68  HCH addition up to 150 mg/L has no negative influence on final methane yield from main

69  substrate and the transformation rates of γ- and α-HCH were high, which demonstrated that AD

70  appears to be a bioremediation option for HCH contaminated biomass.

71  For this work, we scaled up the AD process to bio-transform HCH in continuous mode, for

72  characterization of the transformation processes as required before utilizing contaminated

73  biomass in large-scale for biogas production. Therefore, a continuous stirred tank reactor (CSTR)

74  was established to investigate the interaction of HCHs and microbiota in larger scale in semi-

75  continuous feeding mode.

76  The transformation pathway of HCHs can be identified employing metabolite formation and

77  compound-specific stable isotope analysis (CSIA) [19–22]. Fractionation factors of HCH can

78  then be used for comparison with culture studies for characterisation of the transformation

79  pathway in AD process [23–26]. Moreover, assessment of the main methanogenic pathways in

80  biogas reactors [27–30] can be deduced from isotope composition of the produced methane [31–

4

81  36]. In addition, batch experiment with $^{13}C$-labelled benzene was conducted for investigation of

82  the complete mineralisation of HCHs to $CH_4$ and $CO_2$.

83  Overall, we evaluated the potential application of AD system for treatment of HCH-

84  contaminated biomass in a technical laboratory-scale CSTR. The specific objectives of this study

85  were to: (i) monitor the convential operation of CSTR with addition of HCH isomers (γ, α and

86  β); (ii) prove the potential application of AD for treatment of HCH-contaminated biomass in

87  continuous reactor mode; (iii) characterize the biotransformation pathways of HCHs and the

88  effect of various isomers on microbiota in AD; (iv) show the potential conversion of HCHs to

89  methane and $CO_2$ in AD system.

90  ## 2.  Materials and Methods

91  ### 2.1.    Substrate and Inoculum

92  Maize silage (Total solids (TS) = 25.47%, VS (volatile solids) = 96.51% of TS) was used as

93  substrate. The inoculum (TS = 3.41%, VS = 72.20% TS) was sieved biogas slurry taken from the

94  main reactor of a pilot-scale biogas plant which used maize silage and cattle manure as substrate

95  with an organic loading rate (OLR) of 3.5 $g_{vs}L^{-1}day^{-1}$ and hydraulic retention time (HRT) of 47

96  days. HCH isomers (γ-, α- and β-HCH, separately, analytical purity of 99%) and

97  hexachlorobenzene (HCB) (Lot 60119, analytical purity of 99%), were obtained from Sigma-

98  Aldrich (Munich, Germany). Final concentration of HCH (each isomer) in the reactors was set as

99  50 μM based on the literature value [37] and our previous inhibition experiment [8] to reflect

100  some potential real case scenarios.

5

## 2.2. Setup of CSTRs

Two laboratory-scale CSTRs were operated over more than one year under mesophilic condition

(38-40℃) with maize silage as exclusive substrate. One reactor (reactor R4.36) with HCH

addition was set up to investigate the interaction of HCH with microbiota; another reactor

(reactor R4.35) was operated as the control experiment without addition of HCH. The total

reactor volume was 15 L with 10 L working volume. The whole running period was divided into

4 stages for R4.36 after the start-up: the steady phase for establishing the biogas process (phase

I), the addition of γ-HCH (phase II), the addition of α-HCH (phase III) and the addition of β-

HCH (phase IV) (details of reactor setup see **section A.1.1., Appendix A**).

## 2.3. Sampling procedure and operating parameters analysis of CSTR

The biogas was collected in a gas bag which was connected to a gas meter TG 05 (Ritter,

Germany), then transferred to an AwiFlex gas analyzer (Awite Bioenergie GmbH, Germany) for

gas composition measurement [38]. Biogas samples for isotope analysis were taken from the

headspace of CSTRs weekly before daily addition of maize silage. They were collected in

triplicates using 10-ml gas-tight vacuumed vials for carbon isotope composition [33].

6

116 Effluent liquid was periodically collected from both reactors at the same time: (i) 50 mL liquid

117 were stored in 120 mL serum bottle at -20 ℃ for extraction of HCH and its metabolites, to

118 measure the concentration and carbon isotope composition. The detailed protocol was described

119 in our previous publication [8]. (ii) Another 50 mL were taken weekly and centrifuged at 10,000

120 × g, 10 ℃ for 10 min and filtered with a mesh sieve of 1 mm. The filtrate was used for analysis

121 of volatile fatty acid (VFA) and total ammonia nitrogen (TAN) (details of analysis on parameters

122 see **section A.1.2., Appendix A**).

123 **2.4.    Microbial community structure analysis**

124 Triplicate 0.5 mL samples were taken from both CSTRs periodically and stored at -20 ℃ for

125 molecular biological analysis. Three samplings for each phase with single HCH isomer were

126 conducted (day 129 for steady phase; days 161, 181 and 197 for γ-HCH phase; days 277 and 301

127 for α-HCH phase; days 330, 352 and 378 for β-HCH phase). The total genomic DNA was

7

128 extracted with 'NucleoSpin Soil' kit (Macherey-Nagel GmbH & Co. KG, Düren, Germany)

129 according to the manufacturer's protocol using buffer SL2 with enhancer SX.

130 The 16S rRNA genes were further amplified and sequenced via Illumina[@] MiSeq. Shannon index

131 and amplicon sequence variant (ASV) counts (α-diversity) were determined using the R package

132 phyloseq [39]. Differences in bacterial community composition (β-diversity) were calculated

133 using Bray–Curtis dissimilarity index based on rarefied (15063 ASV counts per sample) and

134 square-root-transformed ASV abundances, which are demonstrated via nonmetric multi-

135 dimensional scaling (NMDS) plot. Permutational multivariate analysis of variance

136 (PERMANOVA) [40] were calculated by "adonis2" function in "vegan" R package using $10^6$

137 permutations to determine if different environmental variables (i.e., time, HCH addition and

138 reactor phases) were important factors correlated with shifts in ASV abundance. Further, ASVs

139 which could be used to classify the difference of HCH-added and non-added reactors between

140 reactor phases were identified (hereafter, bioindicators). In order to determine bioindicators, the

141 analyzes were conducted with three steps [41]. First, machine learning derived from Random

142 Forest [42] to calculate variable important ASVs via Mean Decrease Gini for reactor phase and

143 other important factors from the NMDS analysis. Second, the potential bioindicators were those

144 ASVs that only present on machine learning of reactor phase deducting the ASVs that both

145 relevant for reactor phase and other important factors. Third, bioindicators were identified from

146 the above selected ASVs removing those were not statistically significant via the LSMEANS test

147 with pair-wise methods adjusted by false discovery rate (FDR) correction [43,44].

148 The diversity of microbial communities from both reactors was also investigated by terminal

149 restriction fragment length polymorphism (T-RFLP) analysis of methyl-coenzyme M reductase

8

150 alpha-subunit (*mcrA*) genes for archaea and the variable regions V1–V3 of bacterial 16S rRNA

151 gene fragments for bacteria [45–48].

## 2.5. Batch experiments with labelled benzene-$^{13}C_6$ in AD

153 For evaluating further degradation of the HCH metabolite benzene, labelled compound (benzene-

154 $^{13}C_6$) with final concentration of 100 µM was spiked with a glass syringe as pure compound into

155 serum bottles filled with 50 ml slurry taken from the benzene-added set of automatic methane

156 potential test system (AMPTS, Bioprocess Control Sweden AB, Sweden) described in our

157 previous study [8]. The preparation was done in an anaerobic glove box (gas atmosphere—$N_2:H_2$

158 (95:5); Coy Laboratory Products Inc., USA). Control set was prepared simultaneously in

159 triplicate only with slurry from benzene-added set.

## 2.6. Enantioselectivity and Enantiomer-specific stable isotope fractionation of α-HCH

161 In order to derive enantioselectivity (ES), 21.8 mg/L (75 µmol/L) of α-HCH were added

162 respectively into 120 mL bottles with 50 mL biogas digestate from CSTR effluent. The

163 headspace was flushed with nitrogen for 5 min before the bottles were closed with Teflon™-

164 coated butyl rubber septa and crimped. Fifteen parallel bottles for each isomer were prepared for

165 sampling at different time points. (details on calculation of ES see **section A.1.5., Appendix A**).

166 In addition, triplicate negative controls with sterilized digestate and α-HCH were conducted. In

167 the sterilized control concentration remain stable and no metabolites were detected, showing that

168 biotransformation only occurred in active biogas digestate (data not shown).

9

169 **3. Results**

170 **3.1. Performance of CSTRs**

171 **3.1.1. Methane production, total ammonium nitrogen and volatile fatty acids for**

172 **characterization of AD processes**

173 In phase I (steady phase), the average specific methane production (SMP) was $286 \pm 32.1$ and

174 $283 \pm 27.7$ mL$_N$/g VS in the control reactor and the reactor later used for HCH supplementation,

175 respectively, and were statistically identical. After addition of γ-HCH in phase II, SMPs were

176 $287 \pm 36.5$ and $306 \pm 36.7$ mL$_N$/g VS in the control and HCH-added reactor, respectively; in

177 phase III, the SMPs were $311 \pm 43.2$ and $308 \pm 44.2$ mL$_N$/g VS in control and α-HCH reactors,

178 respectively; in phase IV, SMPs of $266 \pm 31.8$ and $283 \pm 39.4$ mL$_N$/g VS were observed in

179 control and β-HCH reactors, respectively (**Fig. 1a and Table 1**). The SMPs were statistically

180 identical in both reactors during phase I to IV, indicating addition of HCHs did not affect the

181 SMP. Methane and $CO_2$ contents were 54~56% and 43~45%, respectively, during the whole

182 running period (**Fig. 1b**).

183 In start-up phase, concentrations of VFAs and acetate were $95.1 \pm 68.5$ and $66.4 \pm 45.1$ mg/L for

184 control reactor, respectively ($108.4 \pm 81.2$ and $64.8 \pm 42.4$ mg/L for HCH-added reactor). In

185 phase II and III (γ-HCH and α-HCH phase), the concentrations of VFAs and acetate were

186 generally slightly higher in HCH-added reactor compared to the control reactor (**Fig. 1c** and **Fig.**

187 **A.2**). In general, there was a significant difference between concentrations of VFAs in these two

188 reactors (p-value= 0.02187, $p < 0.05$; one way ANOVA analysis), nevertheless all these values

189 were still within conventional ranges of stable operation.

10

### 3.1.2. Concentration and stable isotope analysis for biotransformation of HCHs

Concentrations and stable isotope compositions of HCHs and the metabolites are shown in **Fig. 2**. In phase II (day 147-187), the addition of HCH was about 50 μM for the whole reactor. Both γ- and α-HCH were nearly completely removed within 14 days and 7 days, respectively. The γ-HCH degraded faster after day 173 with a removal below the limit of detection within 3 days. Similarly, in phase III (day 245-275), α-HCH transformed faster at day 253 compared to addition at day 245. In phase II and III, benzene and MCB were detected as metabolites. No transformation of β-HCH was detected in phase IV of our system from day 330 to day 360, which was deduced from the constant concentration and lack of metabolites.

Carbon isotope enrichment of γ-HCH and α-HCH was observed from -27.5 to -21.0‰ and from -27.5 to -24.0‰, respectively (**Fig. 2**). The variations were in a similar order with respect to the isotope enrichment of $\delta^{13}C$ observed in our previous study from -27.5 to -17.0‰ for γ-HCH and from -27.5 to -23.0‰ for α-HCH [8], however the number of data do not allow quantifying the isotope fractionation using the Rayleigh approach in the continuous flow reactor. The $\delta^{13}C$ values of β-HCH were stable at ca. -27.5‰ in phase IV. The $\delta^{13}C$ values of chlorobenzene ranged from -24.8 to -18.2‰ in γ-HCH phase and from -28.1 to -25.1‰ in α-HCH phase, showing same increasing tendency as HCH isomers. Whereas $\delta^{13}C$ values of benzene was ranging from -29.8 to -27.2‰ but the isotope measurement of this metabolite was only possible in few samples, due to the low concentrations (**Fig. 2**).

### 3.1.3. Microbial community structure

NMDS plots for bacterial microbial community structures of all selected samples in both reactors are shown in **Fig. A.5**. In the PERMANOVA main test (**Table A.2**), significant difference (Pseudo-F = 2.25788, P = 0.004693, **Fig. A.5b**) was observed between the two reactors taken the

11

213    reactor phase as a factor. Although, no significant difference was shown between both reactors

214    taking HCH addition as a factor (Pseudo-F = 1.64138, P = 0.095825, **Fig. A.5b**) we observed

215    statistically significant differences when comparing the different reactor phases to the control

216    samples collected in the same dates (**Fig. A.5.c-e**). In addition, time was also found as important

217    factor between early and late phases with the significant difference (Pseudo-F = 9.07219 and P =

218    0.000012) (**Fig. A.5a**). For identification of the bioindicators which could differentiate HCH-

219    added reactor and control reactor responding to reactor phase, three steps were conducted. First,

220    as reactor phase and time both were important factors, 35 variable important ASVs were selected

221    for each of them based on random forest analysis (**Fig. A.6 & A.7**). Moreover, confusion

222    matrices were generated for classification of the samples using the rarefied ASV relative

223    abundances as numeric values with time, HCH-addition and HCH phase as factors (**Table A.1**).

224    Second, 28 ASVs were obtained as potential bioindicators relevant to reactor phase rather than

225    time after machine learning (**Table A.3**). Third, 10 ASVs significantly different ($P < 0.05$) to

226    reactor phase via the LSMEANS test by FDR multiple correction (**Appendix B & C**) selected

227    from last two steps, were identified as bioindicators. Boxplots were used for every chosen

228    bioindicator to depict statistically different ($P < 0.05$) contribution of ASVs caused by addition

229    of different HCH isomer in HCH-added reactor and control reactor (**Fig. A.8**). To demonstrate

230    ASVs which were significantly associated with the pairwise reactor phases ($P < 0.05$) (**Fig. 3**),

231    these ASVs were separated into four groups: steady phase vs. β-HCH phase (Group1); γ-HCH

232    phase vs. α-HCH phase (Group2); γ-HCH phase vs. β-HCH phase (Group3); α-HCH phase vs. β-

233    HCH phase (Group4). Among the 10 ASVs identified as bioindicators, 8 ASVs are classified to

234    order *Clostridiales*, which provide the relations of HCH addition with the abundance of

235    *Clostridiales*. The other 2 ASVs are assigned to order *Hydrogenisporales*.

236 The variation of methanogens in control reactor and HCH-added reactor at different phases was

237 demonstrated via T-RFLP (**Fig. A.9**). The bacterial and archaeal community compositions in

238 both reactors converged toward different direction in intra-sample variability NMDS plots (**Fig.**

239 **A.10**). Significant difference was observed in archaea between the control reactor and HCH-

240 added reactor (PERMANOVA main test; pseudo-F = 2.986, P = 0.015, see also **Fig. A.10a**).

241 However, no significant difference was observed in bacteria from the NMDS plots

242 (PERMANOVA main test; pseudo-F = 2.205, P >0.05, see also **Fig. A.10b**). The correlation

243 between the communities and reactor parameters is depicted as arrows in the NMDS plots. The

244 direction and length of arrow which represents the abundance of genus *Methanosaeta* showed

245 strong correlation with HCH addition. Furthermore, concentration of acetate was also correlated

246 with addition of HCH solution (**Fig. A.2a**).

247 Taking both results from MiSeq and T-RFLP into consideration, HCH-added reactor had a

248 higher abundance of *Methanosaeta* and *Clostridiales* compared to the control reactor. The

249 isotope signature of methane indicates an increase in acetoclastic methanogens, correlating with

250 the increased *Methanosaeta*.

251 **3.2.     Labelled benzene-$^{13}C_6$ degradation in AD system**

252 The further degradation and mineralization of benzene was observed in the microcosms prepared

253 with slurry from a benzene supplemented batch system of our previous study and amended with

254 $^{13}C_6$-labelled benzene. Significant amounts of $^{13}C$ labelled $CO_2$ ($\delta^{13}C$ = +299.0 ± 0.2‰) and

255 methane ($\delta^{13}C$ = 87.3 ± 0.4‰) were detected after 116 days (**Fig. 4**), which is a direct evidence

256 for the conversion of labelled benzene $^{13}C_6$ to $CO_2$ and methane. Meanwhile, in control set the

257 carbon stable isotope composition of methane and $CO_2$ remained stable at -48.8 ± 1.3 ‰ and

258 14.4 ± 0.3 ‰, respectively.

13

259     The slurry from benzene-added set of AMPTS was also sequenced via Illumina[@] MiSeq.

260     Microbes, such as class *Spirochaetes*, class *Epsilonproteobacteria*, order *Thermotogales*, family

261     *Peptococcaceae*, genera *Pelotomaculum* and *Desulfosporosinus*, potentially associated with

262     benzene degradation [49–53] were found in benzene amended slurry from our system (see

263     **Appendix D & E**).

264     **3.3.     Enantiomer fractionation (EF) and enantiomer-specific isotope fractionation of α-**

265        **HCH in batch experiment**

266     In the sterilized control experiment, $\delta^{13}C$ values of (-) and (+) α-HCH were stable at -31.9 ± 0.5

267     and -30.7 ± 0.2‰, respectively; the concentration remained constant at ca. 75 µmol/L, showing

268     that no abiotic transformation took place. In active biogas slurry, $\delta^{13}C$ values of (-) and (+) α-

269     HCH were both enriched, ranging from -32.1 ± 0.4 to -29.3 ± 0.4‰ and from -30.7 ± 0.1 to -26.9

270     ± 0.1‰, respectively (**Fig. 5a**). According to Rayleigh equation, carbon isotope fractionation

271     factors ($\varepsilon_c$) of (+) and (-) *α*-HCH are -4.1 ± 0.3‰ and -4.6 ± 0.4‰, respectively (**Fig. 5c**).

272     Simultaneously, EF of (-) α-HCH increased from 0.50 to 0.56. The degradation kinetics of (-) α-

273     HCH and (+) α-HCH in biogas slurry with values of 0.015 ± 0.001 and 0.020 ± 0.001are shown

274     in **Fig. 5b**, suggesting preferential transformation of (+) α-HCH in AD system. Similar trend was

275     also observed in CSTR and the EF of (-) α-HCH was shifted to 0.57 (**Fig. A.11**). The

276     enantiomeric fractionation was consistent with the enantioselectivity observed in the batch

277     experiment. Thus, (+) α-HCH was preferentially transformed in AD system and can be used as

278     an indicator for biodegradation.

14

## 4. Discussion

### 4.1. Effect of HCHs on the performance of CSTR

The typical concentration of HCH in plants near the HCH dumpsite was found up to 29 $\mu g \cdot g^{-1}$[2]. Concentrations amended in CSTR (50 $\mu$M, equal to 243 $\mu g \cdot g^{-1}$) was higher; however, no significant differences in both SBP and SMP were observed between two reactors in all phases with $P > 0.05$. Control and HCH-added reactor had similar pH, TAN concentrations, as well as the content of methane and $CO_2$; however, relatively higher concentrations of VFAs were detected in the HCH-added reactor, which might be attributed to the addition of HCH. Overall, the conventional parameters in CSTRs had no significant fluctuation caused by HCH-addition at concentration of 50 $\mu$M, indicating the potential for treatment of HCH contaminated biomass in AD system under continuous mode. The quality of the maize silage used as the main substrate for feeding was not constant; therefore, it had also influence on the gas production values, but it affected both reactors in a similar way.

### 4.2. Bioindicators responding to HCH addition in the microbial communities of CSTR

#### 4.2.1. Dynamics of the bacterial community

Reductive dehalogenation has been proven as main pathway of HCHs transformation in AD system [8], suggesting HCHs as electron acceptors can be co-metabolized by microorganisms. Despite the similar process parameters in the experimental and control reactors, addition of respective HCH isomers in different reactor phases had a significant effect on the microbial community structures. The communities were classified with confidence up to Genus level due to the size of the amplicon in this study; however, groups belonging to the same taxonomic/phylogenetic group have similar functions. ASVs belonging to order *Clostridiales*

15

301 were identified as bioindicator responding to HCH-addition, due to the significant variation on

302 abundance. Moreover, ASVs belonging to the class *Dehalococcoidia*, a taxon containing

303 organohalide respiring bacteria [9,54,55], were also found in our system already in the initial

304 phase (see **Appendix D & E**). This highlights the intrinsic potential of the AD microbiota to deal

305 with halogenated compounds. Acetogenic bacteria and *Clostridium* sp. were found to be linked

306 to reductive dehalogenation of HCHs in other studies [56,57]. Reductive dechlorination of

307 Lindane was also detected from cell-free extracts *of Clostridium rectum* [58] and *Clostridium*

308 *sphenoides* [59].

**4.2.2.  Dynamics of the methanogenic community**

310 The dominant methanogens were affiliated to genus *Methanoculleus* in both reactors (**Fig. A.9**).

311 Species affiliated to *Methanoculleus* were dominant methanogens in many biogas-producing

312 reactor systems fed with maize silage and manure [60]. Although this hydrogenotrophic

313 methanogen was predominant in both reactors, the abundance in HCH-added reactor was lower

314 than in control reactor. These small coccoid methanogens are sensitive to detergents, physical

315 and osmotic stresses [61], which might explain the reduced relative abundance of

316 *Methanoculleus* in the experimental reactor after HCHs solution was added.

317 A significant increase of the abundance of genus *Methanosaeta* in the HCH-added reactor was

318 detected, and it is consistent with the bioindicators derived from Miseq analysis and NMDS

319 plots. The enriched $\delta^{13}$C-CH$_4$ caused by β-HCH addition also confirmed the increased abundance

320 of putative acetotrophic methanogens (**Fig. A.9**). It was reported that *Methanosaeta* spp.

321 outcompeted *Methanosarcina* spp.as acetotrophic methanogens when acetate concentrations

322 were lower than 200 mg L$^{-1}$ [62], similar to observations in this study. *Methanosaeta* and

323 *Methanosarcina* spp. were dominant methanogens in anaerobic reactors treating wastewater with

16

324 other halogenated compounds such as tetrachloroethylene and 2-chlorophenol [63,64]. Genus

325 *Methanosaeta* comprises anaerobic, nonmotile, non-sporeforming rods with flat ends in

326 morphology and it can form flexible filaments in a continuous, tubular, proteinaceous sheath for

327 resisting harmful chemical agents [65]. Thus, it was assumed that its cell envelope structure was

328 conducive to resist the toxicity of HCHs, which resulted in increased predominance of

329 *Methanosaeta* in HCH-added reactor.

### 330 4.3. Biodegradation of HCH to biogas

### 331 4.3.1. Biotransformation of HCH to benzene and chlorobenzene in AD

332 In this study, we proved the biotransformation of HCH not only from the decrease in

333 concentration and the detection of metabolites, but also from the stable isotope compositions of

334 HCH and metabolites, which provides a new unambiguous analysis method for

335 biotransformation of chemicals in AD system. In conventional studies, the indication on

336 biodegradation of chemicals was deduced from the reduced concentration during the reaction

337 period, which is a controversial issue since absorption and volatilization of chemicals in AD

338 slurry can also lead to the decrease of concentration. Biotransformation of HCH can be

339 confirmed from the reduced concentration and enriched carbon isotope composition of HCH

340 during $\gamma$ and $\alpha$-HCH reactor phase, as well as from detection of metabolites and the enrichment

341 of carbon isotope composition of chlorobenzene.

### 342 4.3.2. Mineralization of labelled benzene-$^{13}C_6$ to biogas

343 The formation of labelled methane and $CO_2$ from benzene proved that the detected HCH

344 metabolites benzene can be further degraded. The benzene mineralization to $CO_2$ and methane

345 under methanogenic conditions was reported [51,66–68], however were not detected in AD

17

346 systems before. The putative pathway of benzene is proposed starting with the conversion of

347 benzene to phenol by hydroxylation or to toluene by methylation [69] and subsequent

348 transformation to benzoate [70]. Further degradation can be achieved via benzoyl-CoA pathway

349 [71].

350 The conversion of total amount of benzene to $CH_4$ was estimated, to evaluate the contribution of

351 benzene degradation to enhancement on methane yield. If there is 100% conversion of 100 µmol

352 benzene, ca. 9.2 mL methane will be produced. The calculation was based on the equation below

353 [72], which is calculated with $CO_2$ as electron acceptor under methanogenic conditions:

354 …… (**Eq. 2**)

355 In case of current biomass conversion AD systems, a long storage of digestate is required by the

356 authorities to avoid the residual methane production and its negative climate effect. The retention

357 time in such digestate storage facilities usually exceed 100 days, which would provide the time

358 needed to completely degrade the remaining metabolites benzene to biogas.

359 To evaluate the interaction of AD and HCHs, the proposed linked pathways during full

360 degradation of α and γ HCH in biogas-producing system is summarized in **Scheme 1**. AD

361 provided the reductive condition for dehalogenation of HCH with $H_2$ or acetate, produced during

362 fermentation, as electronic donor. Furthermore, the metabolite benzene was mineralized to

363 biogas in AD. HCH with concentration higher than 150 mg/L can cause temporary inhibition on

364 acetoclastic methanogenesis [8]. In CSTR setup, HCH contaminated plants showed no negative

365 influence on methane production. In general, α and γ HCH can be degraded to methane and $CO_2$

366 in AD systems, indicating the positive potential of HCH-contaminated biomass for biogas

367 production not only from plant substrate but also from the contaminant HCH.

18

### 4.4. Structure selectivity of HCHs in anaerobic digestion

### 4.4.1. Diastereoselectivity of HCHs

The isomers of HCHs denoted by Greek letters (α, β, γ, δ, ε, η, and θ, see **section A.1**, **Appendix A**) differ in their axial- equatorial substitution pattern around the ring [73]. In our previous study, it was assumed that transformation mechanism of HCHs in AD system was reductive dehalogenation [8]. In this study, α, β and γ isomers were tested in CSTR system, among which, γ isomer possessing three axial Cl atoms transformed faster than the α isomer with two axial Cl atoms. Subsequently, no transformation of β isomer without axial Cl atom was observed in AD system. Thus, it was assumed that dihaloelimination or anti-periplanar dehydrochlorination occurs to eliminate sequentially chlorine resulting in the final metabolites as chlorobenzene and benzene [8,15,74]. The transformed order of HCH isomers in our study is consistent with the report of Buser *et al* [74]. The results suggest that the transformation rate of HCH in AD system was associated with the number of axial Cl, since axial atoms are easier to be cleaved from the parent compound than equatorial Cl atoms.

### 4.4.2. Enantioselectivity of α-HCH

Enantioselectivity for α-HCH in biogas reactor is significantly different from the aerobic degradation in research by Bashir *et al* [25]. Variation of (EF) (−), from 0.45 to 0.14 in *Sphingobium indicum* strain B90A and 0.50 to 0.24 for *Sphingobium indicum* strain UT26, was discovered, indicating that (-) α-HCH was preferentially degraded in oxic condition [25]. Contrarily, EF (-) changed from 0.50 to 0.56, which was associated with slight preference towards the transformation of (+) α-HCH in our AD system. The ES values of 0.14 is different from the aerobic transformation by *Sphingobium indicum* strain B90A with ES of -0.45 [21]. However, no enantioselectivity of α-HCH during the reductive dehalogenation by the

19

391 *Dehalococcoides mccartyi* strains in anoxic condition was observed [22]. In contrast, the

392 enantio-selectivity in this study is consistent as reported by Buser and Müller with the faster

393 degradation of (+) α-HCH compared to (-)α-HCH in sewage sludge [74].

394 **5. Conclusion and outlook**

395 The addition of HCHs in CSTR showed no negative influence on conventional reactor

396 parameters and methanogenesis at the concentration range found in biomass grown on

397 contaminated areas. The robust microbiota of AD process can adapt to the toxic HCH isomers

398 and even successful biodegrade γ and α isomers. In addition, benzene can be degraded to

399 methane and $CO_2$, deduced from the isotope labelling test, indicating the potential full

400 conversion of HCHs to biogas with long retention time of post digestion. The isotope and

401 enantiomer fractionation can be used to characterize the transformation in AD systems. The

402 isotope fractionation pattern of HCH might be used to evaluate the process and the isotope

403 fractionation pattern of $CH_4$ and $CO_2$ to monitor the status of the AD reactor. In summary,

404 phytoremediation coupled to AD and subsequent fertilization using digestate is a promising

405 strategy for economic use and simultaneous remediation of POPs contaminated lands.

406 **Conflicts of interest**

407 There are no conflicts to declare.

20

421 **Appendix A. Supplementary material**

422 Supplementary material associated with this article can be found, in the online version.

423 **Appendix B. Supplementary Table A.4**

424 Supplementary Table A.4 associated with this article can be found, in the online version.

425 **Appendix C. Supplementary Table A.5**

426 Supplementary Table A.5 associated with this article can be found, in the online version.

427 **Appendix D. Supplementary Table A.6**

428 Supplementary Table A.6 associated with this article can be found, in the online version.

429 **Appendix E. Supplementary Table A.7**

430 Supplementary Table A.7 associated with this article can be found, in the online version.

431 **Appendix F. Xiao Liu et al., 2019; manuscript in review, for review only**

432 **Appendix G. Yaqing Liu et al., 2019; manuscript in review, for review only**

433

21

**Figure captions**

**Fig. 1** Methane yield (a), methane content (b) and total VFAs (c) in CSTRs over phases I to IV. Data were corrected to pressure (101.325 kPa) and standard temperature (273.15 k), thus are reported as normalized milliliters (mLN) per gram of volatile solid (VS).

**Fig. 2** Concentrations and carbon isotope compositions of γ-HCH (a&b), α-HCH (c&d), β-HCH (e&f) and metabolites (chlorobenzene and benzene). Values of 0 indicate that they were below the detection limit. Black arrows mean adjustment of the concentration to 50 µM and blue arrows represent the addition of HCH to 12 µM. Values of $\delta^{13}C$ are associated with concentration and the data below the confidential interval of detection via GC-IRMS are not shown here.

**Fig. 3** Relative abundance distribution of ASVs used as bioindicators in the control CSTR and HCH-added CSTR per sample.

ASVs separated in 4 different groups depending on statistic differences ($P < 0.05$) of abundance using the LSMEANS test with FDR multiple correction, based on the interaction of pairwise reactor phases: steady phase vs. β-HCH phase (Group1); γ-HCH phase vs. α-HCH phase (Group2); γ-HCH phase vs. β-HCH phase (Group3); α-HCH phase vs. β-HCH phase (Group4).

**Fig. 4** Carbon isotope signatures of methane (a) and $CO_2$ (b) in batch experiment with addition of benzene-$^{13}C_6$.

**Fig. 5** Enantiomer fractionation (EF) of (-) α-HCH and carbon isotope compositions of (-) / (+) α-HCH in biogas slurry (batch experiment) (a); the degradation kinetics of (-) α-HCH (◆) and (+) α-HCH (■) in biogas slurry (b); carbon stable isotope enrichment factors of (-) / (+) α-HCH (c).

22

455     **References**

456     [1]     X. Liu, L. Wu, S. Kümmel, H. Richnow, Characterizing the biotransformation of

457             hexachlorocyclohexane in wheat using compound-specific stable isotope analysis and

458             enantiomer fraction analysis, (2019) submitted, see Appendix F, manuscript in review.

459     [2]     L. Wu, Y. Liu, X. Liu, A. Bajaj, M. Sharma, R. Lal, H. Richnow, Isotope fractionation

460             approach to characterize the reactive transport processes governing the fate of

461             hexachlorocyclohexanes at a contaminated site in India, Environ. Int. 132 (2019) 105036.

462     [3]     J. Vijgen, P.C. Abhilash, Y.F. Li, R. Lal, M. Forter, J. Torres, N. Singh, M. Yunus, C.

463             Tian, A. Schäffer, R. Weber, Hexachlorocyclohexane (HCH) as new Stockholm

464             Convention POPs-a global perspective on the management of Lindane and its waste

465             isomers, Environ. Sci. Pollut. Res. 18 (2011) 152–162.

466     [4]     W. Slooff, A. Matthijsen, J. Canton, H. Eerens, C. van Gestel, E. Heijna-Merkus, P.

467             Greve, P. Janssen, J. van Koten-Vermeulen, J. Knoop, Integrated criteria document

468             hexachlorocyclohexanes, 1988.

469     [5]     L. Wu, S. Moses, Y. Liu, J. Renpenning, H.H. Richnow, A concept for studying the

470             transformation reaction of hexachlorocyclohexanes in food webs using multi-element

471             compound-specific isotope analysis, Anal. Chim. Acta. 1064 (2019) 56–64.

472     [6]     S. Hussain, T. Siddique, M. Arshad, M. Saleem, Bioremediation and phytoremediation of

473             pesticides: recent advances, Crit. Rev. Environ. Sci. Technol. 39 (2009) 843–907.

474     [7]     N. Agrawal, S.K. Shahi, An environmental cleanup strategy - microbial transformation of

475             xenobiotic compounds, Int. J. Curr. Microbiol. Appl. Sci. 4 (2015) 429–461.

23

476 [8]   S. Lian, M. Nikolausz, I. Nijenhuis, A.F. Leite, H.H. Richnow, Biotransformation and

477        inhibition effects of hexachlorocyclohexanes during biogas production from contaminated

478        biomass characterized by isotope fractionation concepts, Bioresour. Technol. 250 (2018)

479        683–690.

480 [9]   T. Kaufhold, M. Schmidt, D. Cichocka, M. Nikolausz, I. Nijenhuis, Dehalogenation of

481        diverse halogenated substrates by a highly enriched *Dehalococcoides*-containing culture

482        derived from the contaminated mega-site in Bitterfeld, FEMS Microbiol. Ecol. 83 (2013)

483        176–188.

484 [10]  J. Ye, A. Singh, O.P. Ward, Biodegradation of nitroaromatics and other nitrogen-

485        containing xenobiotics, World J. Microbiol. Biotechnol. 20 (2004) 117–135.

486 [11]  K.J. Rockne, K.R. Reddy, W.T. Street, Bioremediation of contaminated sites, in: Int. e-

487        Conference Mod. Trends Found. Eng. Geotech. Challenges Solut., 2003: pp. 1–22.

488 [12]  I. V. Robles-González, E. Ríos-Leal, I. Sastre-Conde, F. Fava, N. Rinderknecht-Seijas,

489        H.M. Poggi-Varaldo, Slurry bioreactors with simultaneous electron acceptors for

490        bioremediation of an agricultural soil polluted with Lindane, Process Biochem. 47 (2012)

491        1640–1648.

492 [13]  S. Bashir, K.L. Hitzfeld, M. Gehre, H.H. Richnow, A. Fischer, Evaluating degradation of

493        hexachlorcyclohexane (HCH) isomers within a contaminated aquifer using compound-

494        specific stable carbon isotope analysis (CSIA), Water Res. 71 (2015) 187–196.

495 [14]  P.J.M. Middeldorp, M. Jaspers, A.J.B. Zehnder, G. Schraa, Biotransformation of α-, β-, γ-,

496        and δ -hexachlorocyclohexane under methanogenic conditions, Environ. Sci. Technol. 30

497 (1996) 2345–2349.

[15] R. Lal, G. Pandey, P. Sharma, K. Kumari, S. Malhotra, R. Pandey, V. Raina, H.E. Kohler, C. Holliger, C. Jackson, J.G. Oakeshott, Biochemistry of microbial degradation of hexachlorocyclohexane and prospects for bioremediation, Microbiol. Mol. Biol. Rev. 74 (2010) 58–80.

[16] P.J.M. Middeldorp, W. Van Doesburg, G. Schraa, A.J.M. Stams, Reductive dechlorination of hexachlorocyclohexane (HCH) isomers in soil under anaerobic conditions, Biodegradation. 16 (2005) 283–290.

[17] T.P. Baczynski, J. Kurbiel, Identification of operational parameters critical for removal of selected chlorinated pesticides in UASB reactor, Proc. 9th World Congr. Anaerob. Dig. Anaerob. Convers. Sustain. 1 (2001).

[18] P. Bhatt, M.S. Kumar, S.N. Mudliar, T. Chakrabarti, Biodegradation of tech-hexachlorocyclohexane in a upflow anaerobic sludge blanket (UASB) reactor, Bioresour. Technol. 97 (2006) 824–830.

[19] C. Wiegert, Application of two dimensional compound specific carbon-chlorine isotope analyses for degradation monitoring and assessment of organic pollutants in contaminated soil and groundwater, Dr. Thesis, Stock. Univ. (2013).

[20] S.A. Law, T.F. Bidleman, M.J. Martin, Evidence of enantioselective degradation of α-hexachlorocyclohexane in groundwater, Env. Sci Technol. 38 (2004) 1633–1638.

[21] Y. Liu, L. Wu, P. Kohli, R. Kumar, H. Stryhanyuk, I. Nijenhuis, R. Lal, H.-H. Richnow, Enantiomer and carbon isotope fractionation of α-hexachlorocyclohexane by *Sphingobium*

25

518        *indicum strain* B90A and the corresponding enzymes, Environ. Sci. Technol. 53 (2019)

519        8715-8724.

520   [22]   Y. Liu, J. Liu, J. Renpenning, I. Nijenhuis, H.-H. Richnow, Dual C-Cl isotope analysis for

521        characterizing the reductive dechlorination of α- and γ-hexachlorocyclohexane by two

522        *Dehalococcoides mccartyi* strains and an Enrichment culture, (2019) submitted, see

523        Appendix G, manuscript in review.

524   [23]   S.L. Badea, C. Vogt, S. Weber, A.F. Danet, H.H. Richnow, Stable isotope fractionation of

525        γ-hexachlorocyclohexane (Lindane) during reductive dechlorination by two strains of

526        sulfate-reducing bacteria, Environ. Sci. Technol. 43 (2009) 3155–3161.

527   [24]   S.L. Badea, C. Vogt, M. Gehre, A. Fischer, A.F. Danet, H.H. Richnow, Development of

528        an enantiomer-specific stable carbon isotope analysis (ESIA) method for assessing the fate

529        of α-hexachlorocyclohexane in the environment, Rapid Commun. Mass Spectrom. 25

530        (2011) 1363–1372.

531   [25]   S. Bashir, A. Fischer, I. Nijenhuis, H.H. Richnow, Enantioselective carbon stable isotope

532        fractionation of hexachlorocyclohexane during aerobic biodegradation by *Sphingobium*

533        spp., Environ. Sci. Technol. 47 (2013) 11432–11439.

534   [26]   S. Bashir, Assessment of in situ transformation of Hexachlorocyclohexane using carbon

535        stable isotope analysis (CSIA) (Doctoral dissertation), Eberhard Karls Universität

536        Tübingen, 2014.

537   [27]   D. Polag, L.C. Krapf, H. Heuwinkel, S. Laukenmann, J. Lelieveld, F. Keppler, Stable

538        carbon isotopes of methane for real-time process monitoring in anaerobic digesters, Eng.

26

539    Life Sci. 14 (2014) 153–160.

540    [28]    D. Polag, T. May, L. Müller, H. König, F. Jacobi, S. Laukenmann, F. Keppler, Online

541            monitoring of stable carbon isotopes of methane in anaerobic digestion as a new tool for

542            early warning of process instability, Bioresour. Technol. 197 (2015) 161–170.

543    [29]    Z. Lv, M. Hu, H. Harms, H.H. Richnow, J. Liebetrau, M. Nikolausz, H. Hermann, J.

544            Liebetrau, M. Nikolausz, Stable isotope composition of biogas allows early warning of

545            complete process failure as a result of ammonia inhibition in anaerobic digesters,

546            Bioresour. Technol. 167 (2014) 251–259.

547    [30]    J. De Vrieze, M. De Waele, P. Boeckx, N. Boon, Isotope fractionation in biogas allows

548            direct microbial community stability monitoring in anaerobic digestion, Environ. Sci.

549            Technol. 52 (2018) 6704–6713.

550    [31]    J.A. Krzycki, W.R. Kenealy, M.J. Deniro, J.G. Zeikusl, Stable carbon isotope

551            fractionation by *Methanosarcina barkeri* during methanogenesis from acetate, methanol,

552            or carbon dioxide-hydrogen, Appl. Environ. Microbiol. 53 (1987) 2597–2599.

553    [32]    R. Conrad, Quantification of methanogenic pathways using stable carbon isotopic

554            signatures: A review and a proposal, Org. Geochem. 36 (2005) 739–752.

555    [33]    S. Laukenmann, D. Polag, M. Greule, A. Gronauer, Identification of methanogenic

556            pathways in anaerobic digesters using stable carbon isotopes, Eng. Life Sci. 10 (2010)

557            509–514.

558    [34]    P.E. Galand, K. Yrjälä, R. Conrad, Stable carbon isotope fractionation during

559            methanogenesis in three boreal peatland ecosystems, Biogeosciences. 7 (2010) 3893–

560        3900.

561  [35]  H. Penning, P. Claus, P. Casper, R. Conrad, Carbon isotope fractionation during

562        acetoclastic methanogenesis by *Methanosaeta concilii* in culture and a lake sediment,

563        Appl. Environ. Microbiol. 72 (2006) 5648–5652.

564  [36]  E.R.C. Hornibrook, F.J. Longstaffe, W.S. Fyfe, Evolution of stable carbon isotope

565        compositions for methane and carbon dioxide in freshwater wetlands and other anaerobic

566        environments, Geochim. Cosmochim. Acta. 64 (2000) 1013–1027.

567  [37]  J.C. Quintero, M.T. Moreira, J.M. Lema, G. Feijoo, An anaerobic bioreactor allows the

568        efficient degradation of HCH isomers in soil slurry, Chemosphere. 63 (2006) 1005–1013.

569  [38]  D.G. Mulat, H.F. Jacobi, A. Feilberg, A.P.S. Adamsen, H.-H. Richnow, M. Nikolausz,

570        Changing feeding regimes to demonstrate flexible biogas production: effects on process

571        performance, microbial community structure, and methanogenesis pathways, Appl.

572        Environ. Microbiol. 82 (2016) 438–449.

573  [39]  P.J. McMurdie, S. Holmes, phyloseq: an R package for reproducible interactive analysis

574        and graphics of microbiome census data, PLoS One. 8 (2013) 1–11.

575  [40]  M.J. Anderson, Permutational multivariate analysis of variance (PERMANOVA), Wiley

576        StatsRef Stat. Ref. Online. (2017) 1–15.

577  [41]  P.M. Rosado, D.C.A. Leite, G.A.S. Duarte, R.M. Chaloub, G. Jospin, U. Nunes da Rocha,

578        J. P. Saraiva, F. Dini-Andreote, J.A. Eisen, D.G. Bourne, R.S. Peixoto, Marine probiotics:

579        increasing coral resistance to bleaching through microbiome manipulation, ISME J.

580        (2018) Published: 05 December 2018.

581 [42] A. Liaw, M. Wiener, Classification and regression by randomForest, R News. 2/3 (2002)

582    18–22.

583 [43] A. V. Longo, K.R. Zamudio, Environmental fluctuations and host skin bacteria shift

584    survival advantage between frogs and their fungal pathogen, ISME J. 11 (2017) 349–361.

585 [44] R. V. Lenth, Least-squares means: the R package lsmeans, J. Stat. Softw. 69 (2016) 1–33.

586 [45] T. Lueders, K.J. Chin, R. Conrad, M. Friedrich, Molecular analyses of methyl-coenzyme

587    M reductase α-subunit (*mcrA*) genes in rice field soil and enrichment cultures reveal the

588    methanogenic phenotype of a novel archaeal lineage, Environ. Microbiol. 3 (2001) 194–

589    204.

590 [46] J.D. Neufeld, W.W. Mohn, V. De Lorenzo, Composition of microbial communities in

591    hexachlorocyclohexane (HCH) contaminated soils from Spain revealed with a habitat-

592    specific microarray, Environ. Microbiol. 8 (2006) 126–140.

593 [47] N. Sangwan, P. Lata, V. Dwivedi, A. Singh, N. Niharika, J. Kaur, S. Anand, J. Malhotra,

594    S. Jindal, A. Nigam, D. Lal, A. Dua, A. Saxena, N. Garg, M. Verma, J. Kaur, U.

595    Mukherjee, J.A. Gilbert, S.E. Dowd, R. Raman, P. Khurana, J.P. Khurana, R. Lal,

596    Comparative metagenomic analysis of soil microbial communities across three

597    hexachlorocyclohexane contamination levels, PLoS One. 7 (2012) 1–12.

598 [48] M.J. Whiticar, E. Faber, M. Schoell, Biogenic methane formation in marine and

599    freshwater environments: $CO_2$ reduction vs acetate fermentation - isotope evidence,

600    Geochim. Cosmochim. Acta. 50 (1986) 693–709.

601 [49] M. Nales, B.J. Butler, E.A. Edwards, Anaerobic benzene biodegradation: a microcosm

602      survey, Bioremediat. J. 2 (1998) 125–144.

603 [50] J.N. Rooney-varga, R.T. Anderson, J.L. Fraga, D.R. Lovley, Microbial communities

604      associated with anaerobic benzene degradation in a petroleum-contaminated aquifer,

605      Appl. Environ. Microbiol. 65 (1999) 3056–3063.

606 [51] C. Vogt, S. Kleinsteuber, H.H. Richnow, Anaerobic benzene degradation by bacteria,

607      Microb. Biotechnol. 4 (2011) 710–724.

608 [52] S. Atashgahi, B. Hornung, M.J. van der Waals, U. Nunes da Rocha, F. Hugenholtz, B.

609      Nijsse, D. Molenaar, R. van Spanning, A.J.M. Stams, J. Gerritse, H. Smidt, A benzene-

610      degrading nitrate-reducing microbial consortium displays aerobic and anaerobic benzene

611      degradation pathways, Sci. Rep. (2018) 1–12.

612 [53] M.J. van der Waals, C. Pijls, A.J.C. Sinke, A.A.M. Langenhoff, H. Smidt, J. Gerritse,

613      Anaerobic degradation of a mixture of MtBE, EtBE, TBA, and benzene under different

614      redox conditions, Appl. Microbiol. Biotechnol. 102 (2018) 3387–3397.

615 [54] B. Matturro, C. Ubaldi, S. Rossetti, Microbiome dynamics of a polychlorobiphenyl (PCB)

616      historically contaminated marine sediment under conditions promoting reductive

617      dechlorination, Front. Microbiol. 7 (2016) 1–14.

618 [55] S. Bashir, K. Kuntze, C. Vogt, I. Nijenhuis, Anaerobic biotransformation of

619      hexachlorocyclohexane isomers by *Dehalococcoides* species and an enrichment culture,

620      Biodegradation. 29 (2018) 409–418.

621 [56] B. Camacho-Pérez, E. Ríos-Leal, N. Rinderknecht-Seijas, H.M. Poggi-Varaldo, Enzymes

622      involved in the biodegradation of hexachlorocyclohexane: a mini review, J. Environ.

30

623        Manage. 95 (2012) S306–S318.

624    [57]    C. Holliger, G. Schraa, Physiological meaning and potential for application of reductive

625        dechlorination by anaerobic bacteria, FEMS Microbiol. Rev. 15 (1994) 297–305.

626    [58]    N. Ohisa, M. Yamaguchil, N. Kurihara, Lindane degradation by cell-free extracts of

627        Clostridium rectum, Arch. Microbiol. 225 (1980) 221–225.

628    [59]    A.D. Heritage, I.C. Macrae, Degradation of Lindane by cell-free preparations of

629        *Clostridium sphenoides*, Appl. Environ. Microbiol. 34 (1977) 222–224.

630    [60]    I. Maus, D. Wibberg, R. Stantscheff, F.G. Eikmeyer, A. Seffner, J. Boelter, R.

631        Szczepanowski, J. Blom, S. Jaenicke, H. König, A. Pühler, A. Schlüter, Complete genome

632        sequence of the hydrogenotrophic, methanogenic archaeon *Methanoculleus bourgensis*

633        strain MS2T, isolated from a sewage sludge digester, J. Bacteriol. 194 (2012) 5487–5488.

634    [61]    G.M. Maestrojuán, D.R. Boone, L. Xun, R.A. Mah, L. Zhang, Transfer of

635        *Methanogenium bourgens*e, *Methanogenium marisnigri*, *Methanogenium olentangyi*, and

636        *Methanogenium thermophilicum* to the genus *Methanoculleus* gen. nov., emendation of

637        *Methanoculleus marisnigri* and *Methanogenium*, and description of new strains of

638        *Methanoculleus bourgense* and *Methanoculleus marisnigri*., Int. J. Syst. Bacteriol. 40

639        (2009) 117–122.

640    [62]    D. Zheng, L. Raskin, Quantification of *Methanosaeta* species in anaerobic bioreactors

641        using genus- and species-specific hybridization probes, Microb. Ecol. 39 (2000) 246–262.

642    [63]    S.M. Prakash, S.K. Gupta, Biodegradation of tetrachloroethylene in upflow anaerobic

643        sludge blanket reactor, Bioresour. Technol. 72 (2000) 47–54.

31

644   [64]   L. Beristain-Montiel, S. Martínez-Hernández, F. de M. Cuervo-López, F. Ramírez-Vives,

645         Dynamics of a microbial community exposed to several concentrations of 2-chlorophenol

646         in an anaerobic sequencing batch reactor, Environ. Technol. 36 (2015) 1776–1784.

647   [65]   Girishchandra B. Patel, G.D. Sprott, *Methanosaeta concilii* gen. nov., sp. nov.

648         ("*Methanothrix concilii*") and *Methanosaeta thermoacetophila* nom, rev., comb. nov., Int.

649         J. Syst. Bacteriol. 40 (1990) 79–82.

650   [66]   J. Kazumi, M.E. Caldwell, J.M. Suflita, D.R. Lovley, L.Y. Young, Anaerobic degradation

651         of benzene in diverse anoxic environments, Environ. Sci. Technol. 31 (1997) 813–818.

652   [67]   X. Liang, C.E. Devine, J. Nelson, B. Sherwood Lollar, S. Zinder, E.A. Edwards,

653         Anaerobic conversion of chlorobenzene and benzene to $CH_4$ and $CO_2$ in bioaugmented

654         microcosms, Environ. Sci. Technol. 47 (2013) 2378–2385.

655   [68]   M. Schmidt, D. Wolfram, J. Birkigt, J. Ahlheim, H. Paschke, H.H. Richnow, I. Nijenhuis,

656         Iron oxides stimulate microbial monochlorobenzene in situ transformation in constructed

657         wetlands and laboratory systems, Sci. Total Environ. 472 (2014) 185–193.

658   [69]   S.A. Mancini, C.E. Devine, M. Elsner, M.E. Nandi, A.C. Ulrich, E.A. Edwards, B.S.

659         Lollar, Isotopic evidence suggests different initial reaction mechanisms for anaerobic

660         benzene biodegradation, Environ. Sci. Technol. 42 (2008) 8290–8296.

661   [70]   M.E. Caldwell, J.M. Suflita, Detection of phenol and benzoate as intermediates of

662         anaerobic benzene biodegradation under different terminal electron-accepting conditions,

663         Environ. Sci. Technol. 34 (2000) 1216–1220.

664   [71]   C.S. Harwood, G. Burchhardt, H. Herrmann, G. Fuchs, Anaerobic metabolism of aromatic

665      compounds via the benzoyl-CoA pathway, FEMS Microbiol. Rev. 22 (1998) 439–458.

666   [72]   J.M. Weiner, D.R. Lovley, Rapid benzene degradation in methanogenic sediments from a

667      petroleum-contaminated aquifer, Appl. Environ. Microbiol. 64 (1998) 1937–1939.

668   [73]   K.L. Willett, E.M. Ulrich, R.A. Hites, Differential toxicity and environmental fates of

669      hexachlorocyclohexane isomers, Environ. Sci. Technol. 32 (1998) 2197–2207.

670   [74]   H.R. Buser, M.D. Müller, Isomer and enantioselective degradation of

671      hexachlorocyclohexane isomers in sewage sludge under anaerobic conditions, Environ.

672      Sci. Technol. 29 (1995) 664–672.

| Phase | Reactor | HCH addition | SBP (mL$_N$/g VS) | SMP (mL$_N$/g VS) | Methane (%) | CO$_2$ (%) | pH | TAN (NH$_4^+$-N/L) | VFAs (mg/L) | Acetate (mg/L) | δ$^{13}$C-CH$_4$ (‰) | δ$^{13}$C-CO$_2$ (‰) |
|---|---|---|---|---|---|---|---|---|---|---|---|---|
| Phase I (day 90-150) | R4.35 | no | 511 ± 57.7 | 286 ± 32.1 | 55.9 ± 2.1 | 43.7 ± 2.2 | 7.41 ± 0.09 | 1.90 ± 0.17 | 95.14 ± 68.54 | 66.38 ± 45.07 | -35.7 ± 1.2 | 11.7 ± 0.5 |
| | R4.36 | no | 505 ± 51.2 | 283 ± 27.7 | 55.9 ± 1.9 | 43.8 ± 2.0 | 7.41 ± 0.08 | 1.90 ± 0.17 | 108.37 ± 81.21 | 64.84 ± 42.42 | -34.9 ± 1.2 | 11.9 ± 0.8 |
| Phase II (day 150-240) | R4.35 | no | 555 ± 62.3 | 306 ± 36.7 | 55.0 ± 1.7 | 44.7 ± 1.7 | 7.41 ± 0.13 | 2.14 ± 0.07 | 83.66 ± 38.44 | 56.03 ± 27.80 | -35.6 ± 2.4 | 13.3 ± 0.7 |
| | R4.36 | γ-HCH (50 µM) | 536 ± 66.1 | 287 ± 36.5 | 55.5 ± 1.4 | 44.2 ± 1.4 | 7.42 ± 0.10 | 2.02 ± 0.17 | 155.72 ± 78.27 | 89.70 ± 37.71 | -34.9 ± 1.5 | 11.9 ± 0.9 |
| Phase III (day 240-330) | R4.35 | no | 557 ± 73.9 | 311 ± 43.2 | 55.7 ± 1.8 | 43.9 ± 1.9 | 7.50 ± 0.07 | 2.22 ± 0.05 | 55.21 ± 23.32 | 37.47 ± 13.48 | -33.2 ± 2.5 | 12.6 ± 1.4 |
| | R4.36 | α-HCH (50 µM) | 568 ± 77.0 | 308 ± 44.2 | 55.8 ± 1.6 | 43.8 ± 1.7 | 7.49 ± 0.07 | 2.15 ± 0.10 | 183.64 ± 91.82 | 98.48 ± 36.41 | -34.2 ± 2.9 | 12.3 ± 1.5 |
| Phase IV (day 330-380) | R4.35 | no | 507 ± 67.6 | 266 ± 31.8 | 54.9 ± 2.2 | 44.5 ± 2.6 | 7.52 ± 0.14 | 2.22 ± 0.03 | 216.92 ± 35.82 | 117.40 ± 8.54 | -36.9 ± 2.9 | 13.3 ± 1.6 |
| | R4.36 | β-HCH (50 µM) | 545 ± 87.4 | 283 ± 39.4 | 55.4 ± 2.0 | 44.0 ± 2.4 | 7.56 ± 0.11 | 2.20 ± 0.04 | 151.60 ± 128.19 | 79.98 ± 61.47 | -34.5 ± 6.5 | 13.7 ± 1.2 |

674 **Table 1** Operating conditions and parameters of CSTRs

675

35

676

**Fig. 1** Methane yield (a), methane content (b) and total VFAs (c) in CSTRs over phases I to IV. Data were corrected to pressure (101.325 kPa) and standard temperature (273.15 k), thus are reported as normalized milliliters ($mL_N$) per gram of volatile solid (VS).

**Fig. 2** Concentrations and carbon isotope compositions of $\gamma$-HCH (a&b), $\alpha$-HCH (c&d), $\beta$-HCH (e&f) and metabolites (chlorobenzene and benzene). Values of 0 indicate that they were below the detection limit. Black arrows mean adjustment of the concentration to 50 $\mu$M and blue arrows represent the addition of HCH to 12 $\mu$M. Values of $\delta^{13}C$ are associated with concentration and the data below the confidential interval of detection via GC-IRMS are not shown here.
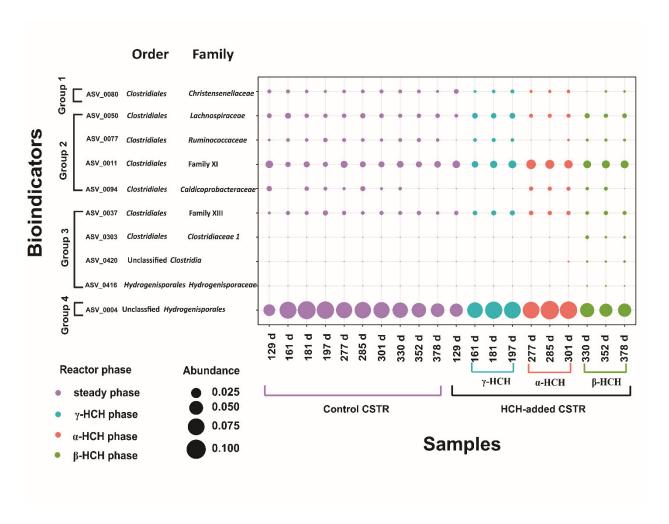
685

**Fig. 3** Relative abundance distribution of ASVs used as bioindicators in the control CSTR and HCH-added CSTR.

ASVs separated in 4 different groups depending on statistic differences ($P < 0.05$) of abundance using the LSMEANS test with FDR multiple correction, based on the interaction of pairwise reactor phases: steady phase vs. β-HCH phase (Group1); γ-HCH phase vs. α-HCH phase (Group2); γ-HCH phase vs. β-HCH phase (Group3); α-HCH phase vs. β-HCH phase (Group4).

37

694     **Fig. 4** Carbon isotope signatures of methane (a) and $CO_2$ (b) in batch experiment with addition

695     of benzene-$^{13}C_6$.

696

697 **Fig. 5** Enantiomer fractionation (EF) of (-) α-HCH and carbon isotope compositions of (-) / (+)

698 α-HCH in biogas slurry (batch experiment) (a); the degradation kinetics of (-) α-HCH (◆) and

699 (+) α-HCH (■) in biogas slurry (b); carbon stable isotope enrichment factors of (-) / (+) α-HCH

700 (c).

701 **Scheme 1** Proposed interaction between anaerobic digestion and HCH dehalogenation with

702 subsequent mineralization



703